Nondestructive, *in situ*, cellular-scale mapping of elemental abundances including organic carbon in permineralized fossils

C. K. Boyce*†, R. M. Hazen‡, and A. H. Knoll*

*Botanical Museum, Harvard University, Cambridge, MA 02138; and ‡Carnegie Geophysical Laboratory, 5251 Broad Branch Road NW, Washington, DC 20015-1305

Contributed by A. H. Knoll, March 16, 2001

The electron microprobe allows elemental abundances to be mapped at the μm scale, but until now high resolution mapping of light elements has been challenging. Modifications of electron microprobe procedure permit fine-scale mapping of carbon. When applied to permineralized fossils, this technique allows simultaneous mapping of organic material, major matrix-forming elements, and trace elements with μm-scale resolution. The resulting data make it possible to test taphonomic hypotheses for the formation of anatomically preserved silicified fossils, including the role of trace elements in the initiation of silica precipitation and in the prevention of organic degradation. The technique allows one to understand the localization of preserved organic matter before undertaking destructive chemical analyses and, because it is nondestructive, offers a potentially important tool for astrobiological investigations of samples returned from Mars or other solar system bodies.

Permineralized fossils preserve biological remains in three-dimensional cellular detail, enabling paleontologists to document the morphology and anatomy of ancient organisms that range from cyanobacteria (1) and the embryos of early animals (2, 3) to both sporophytes and gametophytes of early land plants (4–6). The anatomical resolution provided by permineralized fossils presents opportunities for fine-scale chemical analysis of preserved organic matter, paving the way toward cell- and tissue-level studies of paleobiochemistry (7–10). Maps of elemental abundances at comparable resolution can further facilitate improved understanding of the diagenetic processes that frame these exceptional windows on past biology (11). In addition, the ability to map carbon and other elemental abundances accurately and nondestructively at the μm-scale will be central to astrobiological investigations of samples returned from Mars and elsewhere.

The electron microprobe has the potential to provide information on elemental composition at the μm scale. The electron probe measures the frequency and intensity of x-rays emitted by a sample upon excitation with a beam of electrons. Bombardment with an electron beam results in the ejection of electrons from atoms near the sample surface. Replacement of electron vacancies in the inner valence shells results in x-ray emission, and each element produces a characteristic x-ray spectrum. Comparison of x-ray intensity to standards of known composition allows semiquantitative measurement of elemental abundances. To date, however, high resolution x-ray detection of light elements has been challenging because of the relatively long wavelengths of their characteristic x-rays, lower x-ray yield, and greater x-ray absorption within the sample and its conductive coating (12). In consequence, accurate, fine-scale mapping of carbon abundances in fossils has been difficult to achieve.

Here we describe a modification of standard electron microprobe analytical technique that facilitates nondestructive, *in situ* mapping of elemental abundances, including organic carbon, at the μm scale in anatomically preserved fossils. The ability to map simultaneously the distribution of major and trace elements of the matrix along with the organic carbon of the fossil allows the assessment of taphonomic processes, including the role organic material played in the deposition of the minerals in which it is preserved. Additionally, this technique provides an essential, nondestructive assessment of the quantity, location, and, therefore, likely source of organic carbon before destructive isotopic or organic assays of fossil chemistry are undertaken.

Methods

Fossils used in this study range from Proterozoic cyanobacteria to Neogene angiosperms (see Table 1); in general, vascular plant stems were favored because of the richness of spatial information in anatomical sections. All fossils were preserved by early diagenetic silicification, and all display fine cellular detail when viewed by optical microscopy. We used standard rectangular 1" × 2" or circular 1" polished thin- and thick-sections in microprobe analyses.

Semiquantitative analyses and composition maps of elemental abundances were obtained by using a JEOL 8900 electron microprobe with five wavelength dispersive spectrometers for qualitative maps of elemental composition and an energy dispersive spectrometer for semiquantitative point measurements of elemental abundance. Analyses were performed at 15 keV.

Two modifications of standard microprobe procedures (12) enhanced the detection and spatial resolution of carbon present in low concentrations. The first modification was an increased electron beam current of ≈300 nA, rather than the usual 10 to 30 nA. The higher beam current increases the sensitivity of detection for all elements, but is particularly important for detecting small amounts of light elements, including carbon, which produce characteristic x-rays with low efficiency.

The second modification was the use of aluminum-coated rather than carbon-coated samples, achieved by placing a 1 cm × 1 cm square of aluminum foil into the tungsten wire holder of a vacuum coating device. The aluminum was vaporized by passing current through the tungsten wire. Aluminum was chosen because it is the lightest metallic element that is cheap, stable, and safe, allowing good conductance without high absorbance of electrons—a problem for heavier metal coatings (examples in ref. 12). Aluminum coating dissipates the increased beam current more effectively than carbon coating. Use of aluminum also eliminates a key problem of carbon coats: discrimination between carbon in the coat itself and carbon native to the sample.

Results

As shown in elemental analyses illustrated here, our modified electron microprobe technique maps carbon accurately at the cellular level. In the best-preserved samples, the microprobe data dramatically confirm the correspondence of organic carbon

†To whom reprint requests should be addressed. E-mail: cboyce@oeb.harvard.edu.

The publication costs of this article were defrayed in part by page charge payment. This article must therefore be hereby marked "*advertisement*" in accordance with 18 U.S.C. §1734 solely to indicate this fact.

Table 1. Silicified material examined for this study

Formation (ref.)	Location	Age
Draken Formation (13)	Spitsbergen	Neoproterozoic
Rhynie Chert (14)	Scotland	Early Devonian
Olentangy Shale (15)	Ohio	Early Carboniferous
Serian Volcanic Formation (16)	Sarawak	Late Triassic
Morrison Formation (17)	Utah	Jurassic
Princeton Chert (18)	Alberta	Eocene
Vantage Sandstone (19, 20)	Washington	Miocene
Lost Chicken Creek Chert (1)	Alaska	Miocene/Pliocene

with cell walls: Fig. 1 shows carbon distribution in preserved tracheids of the Devonian lycopod *Asteroxylon*; Fig. 2 maps carbon in spores within the sporangium of an unidentified plant from the same locality. In other samples with equally fine anatomical preservation and often from the same localities, however, microprobe analyses reveal either no carbon or only μm-scale blebs of carbon distributed sporadically along the former locations of cell walls (Figs. 3 and 4). In these latter samples, carbon distribution reflects anatomy, but in a patchy way (Fig. 3). In still other instances, high organic carbon concentrations were found in matrix silica not associated with recognizable biological structures (examples in Fig. 5), potentially complicating the interpretation of any bulk organic geochemical analysis.

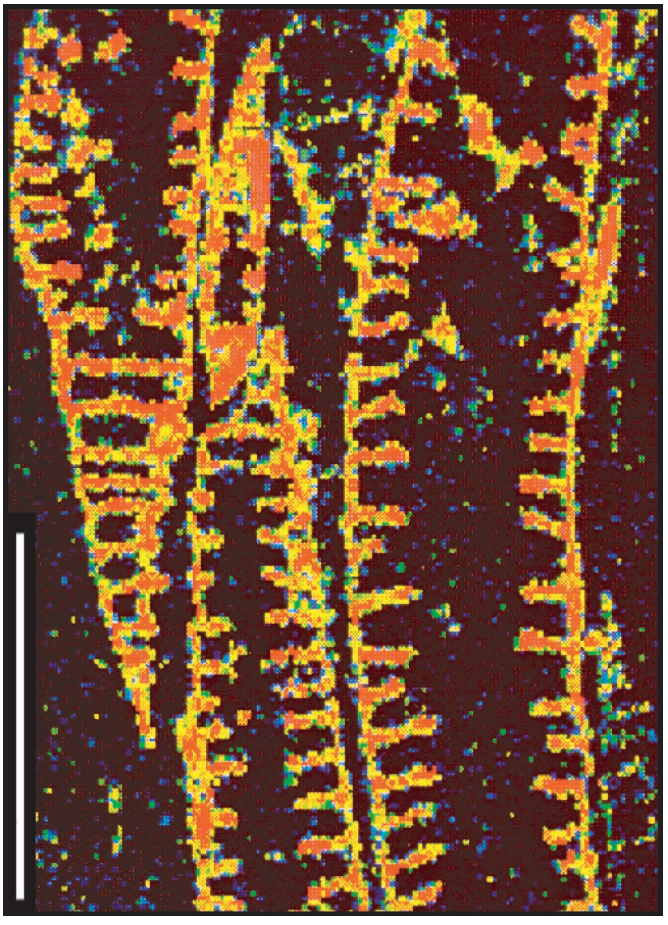

Fig. 1. Carbon elemental map of *Asteroxylon* tracheids from the Devonian Rhynie Chert. In all figures, relative elemental abundances are indicated by color spectrum, with black to blue representing the lowest and red to white the highest abundances. (Scale bar, 100 μm.)

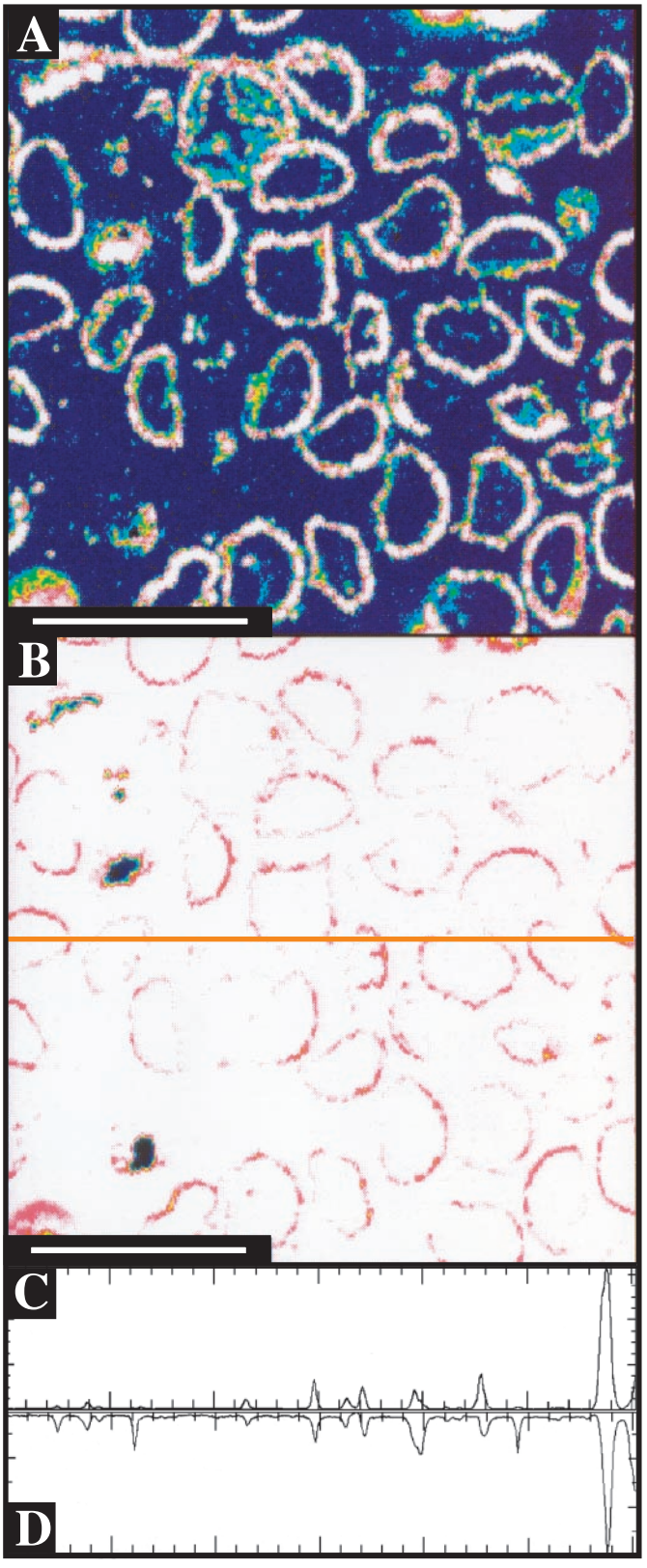

Fig. 2. Spores within a sporangium of unknown affinity from the Rhynie Chert. (*A*) Carbon map. (*B*) Silicon map; orange line is approximate location of transect in *C* and *D*. (*C*) Carbon abundance along transect, scale ranging from 0 to 1,200 counts. (*D*) Silicon abundance along transect, scale ranging from 120,000 to 240,000 counts. (Scale bars, 100 μm.)

GEOLOGY

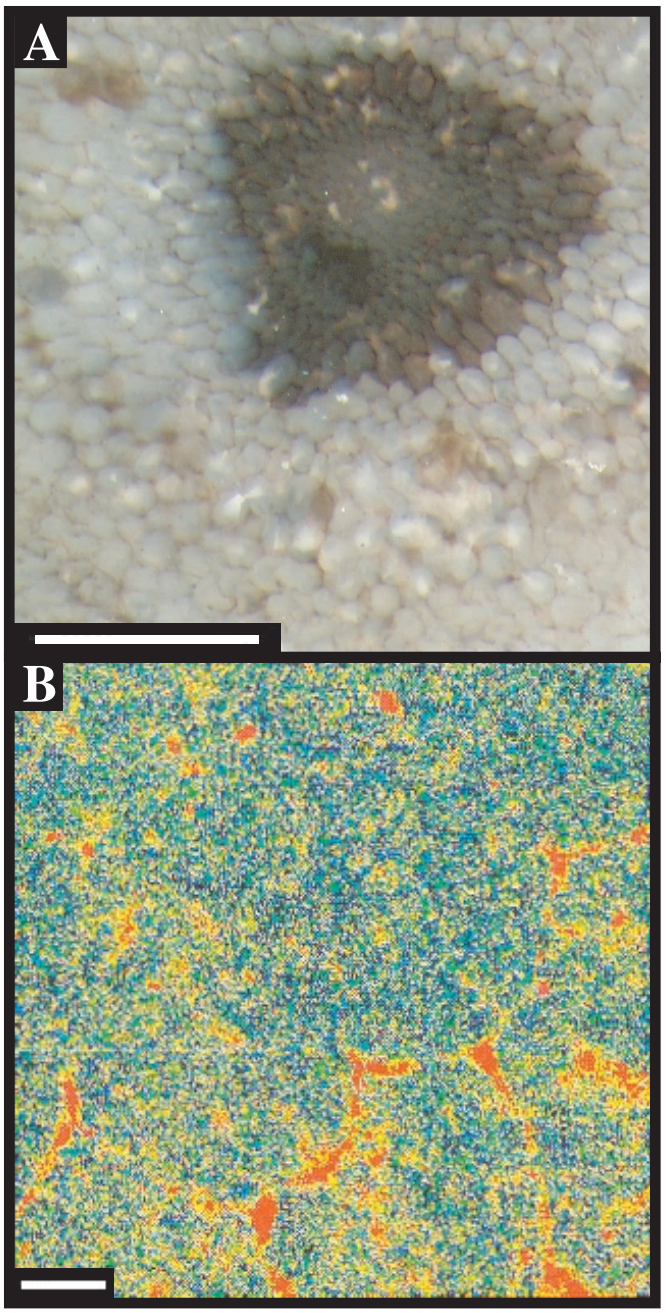

Fig. 3. Cellular preservation in an *Aglaophyton* stem from the Rhynie Chert. (*A*) Microscope image, 0.5 mm scale. (*B*) Elemental map showing patchy preservation of carbon in cell walls, 20 μm scale.

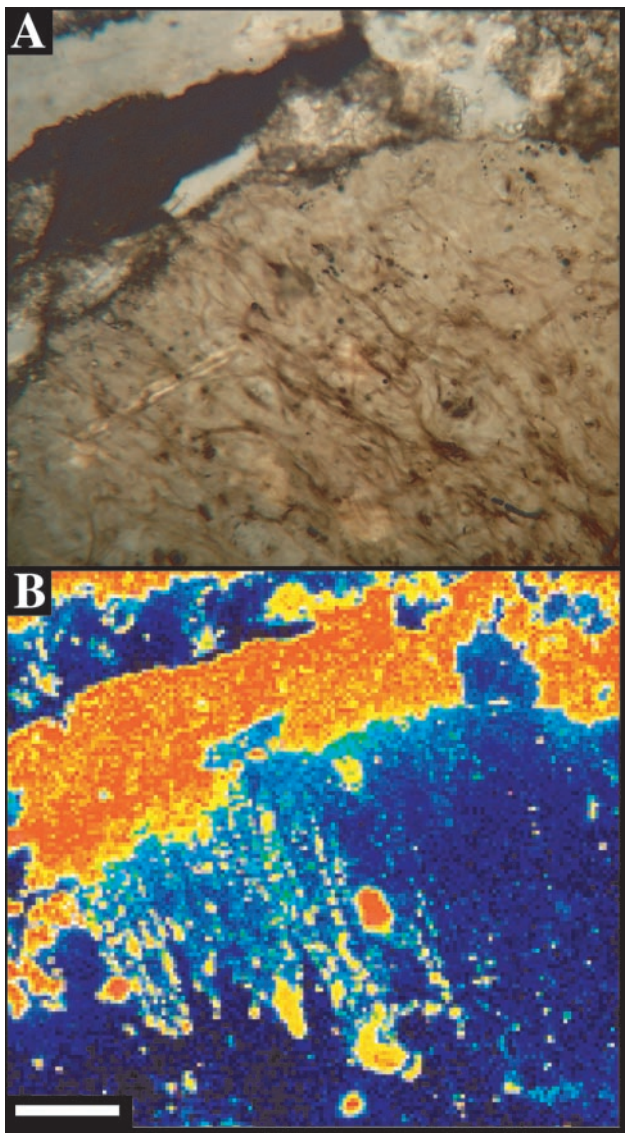

Fig. 4. Cyanobacterial filaments from the Neoproterozoic Draken Formation. (*A*) Microscope image. (*B*) Carbon map. High carbon concentration in upper half of image reflects carbonate matrix surrounding silicified clast containing fossils. (Scale bars, 100 μm.)

In our permineralized samples, organically preserved cell walls are always extensively infiltrated with silica; typically, probe measurements show that silica constitutes 70% or more of the material within preserved cell walls. These concentrations are approximate and may be exaggerated somewhat by averaging of measurements over the 1–3-μm beam width and by the possibility of background x-ray fluorescence over a radius from three to five microns of the surrounding matrix (12). Regardless of these caveats, however, silica is still measured as 50% of the material in the centers of spore walls 8 to 10 microns thick (Fig. 2).

Elevated levels of trace elements are commonly associated with organic material; these include sulfur, calcium, or sodium, depending on locality (see, for example, carbon and sulfur maps of Cenozoic conifer needles in Fig. 5 and carbon, calcium, and sulfur maps of Paleozoic wood in Fig. 6). In some cases, trace elements may clearly define anatomy even when carbon is absent. In the Miocene wood illustrated in Fig. 7, carbon is present only in low background levels that do not reflect anatomy, but calcium maps show clear cellular detail. In this case, the calcium levels were slightly elevated in cell lumens relative to the former locations of cell walls (Fig. 7). Iron was not associated with organic concentrations in any sample (for example, Fig. 5).

Discussion

Silica permineralization has been modeled in terms of the permeation and encrustation of an organic template by silica supplied by silicate ions in solution (21); the absence of organic material in many permineralizations is thought to indicate secondary mineralization following the eventual oxidation of templating organic materials (22). Our observations provide qualitative support for these hypotheses. In organic-free samples

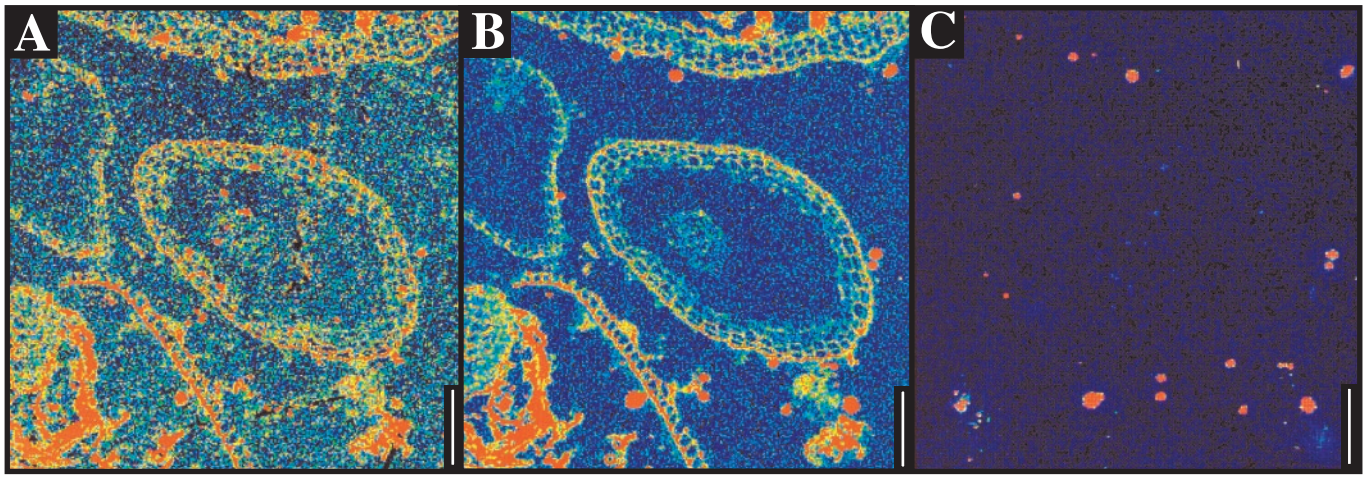

Fig. 5. Conifer needles from the Miocene/Pliocene Lost Chicken Creek Formation. (*A*) Carbon map. Note carbon concentrations without any recognizable biological detail in the bottom half of the figure. (*B*) Sulfur map. (*C*) Iron map. (Scale bars, 100 μm.)

of petrified wood (Fig. 7), trace element chemistry differs between the silica that fills cell cavities and that marking the former position of cell walls; this difference suggests multiple episodes of mineralization with intervening organic degradation, rather than primary replacement of organic materials at the time of lumen infilling.

Observations from silicified bacteria in modern marine hydrothermal vents and experimental analyses in laboratory settings have suggested that metal cations, particularly iron, may play an important role in the adsorption of silica on cell surfaces by providing a bridge between negative sites on the organic surface and silicate anions (23, 24). Although pyrite grains are often present in the matrices of our samples and occasionally occur, as well, in spaces within fossils, iron is not associated with organic material in fossils from any locality included in this study (Fig. 5). This does not necessarily lessen the importance of iron in the preservation of microorganisms in silica-rich hot spring environments, but it does suggest that iron chelation is not a universal requirement for silica permineralization. Trace amounts of calcium, insufficient to account for the carbon as carbonate, are commonly associated with organic material in our samples (Fig. 6), and it is possible that in these instances calcium served as a cation bridge between organic and silicate anions during permineralization. No single trace element is universally present, however, and it may be that calcium and other trace elements, such as sodium, were passive participants that simply recorded aspects of the fluid environment of fossilization that were otherwise excluded from the microcrystalline quartz matrix.

Sulfur is also commonly found in association with organics in our samples (Figs. 5 and 6). In siliciclastic depositional environments, it has been demonstrated that sulfur is incorporated into alkenes during diagenesis; the sequestration of organics into macromolecular complexes by the formation of intramolecular sulfur-linkages may play a role in protecting organic materials from degradation (25, 26). This may contribute to the preferential preservation of cell walls impregnated with lignins and sporopollenins, which are rich in carbon–carbon double bonds, over primary cell walls comprised largely of cellulose, hemicellulose, and pectins, which are devoid of double bonds. In the future, it may be possible to take advantage of this preferential incorporation of sulfur into alkenes by using the sulfur to carbon abundance ratio in organically preserved cell walls as an indication of the types of cell wall compounds that were originally present.

An alternative explanation for the organic associated trace element chemistry is that the presence of both sulfur and calcium are the result of organic decomposition mediated by bacterial sulfate reduction and the resulting carbonate deposition (27). However, the absence of any evidence of organic-associated

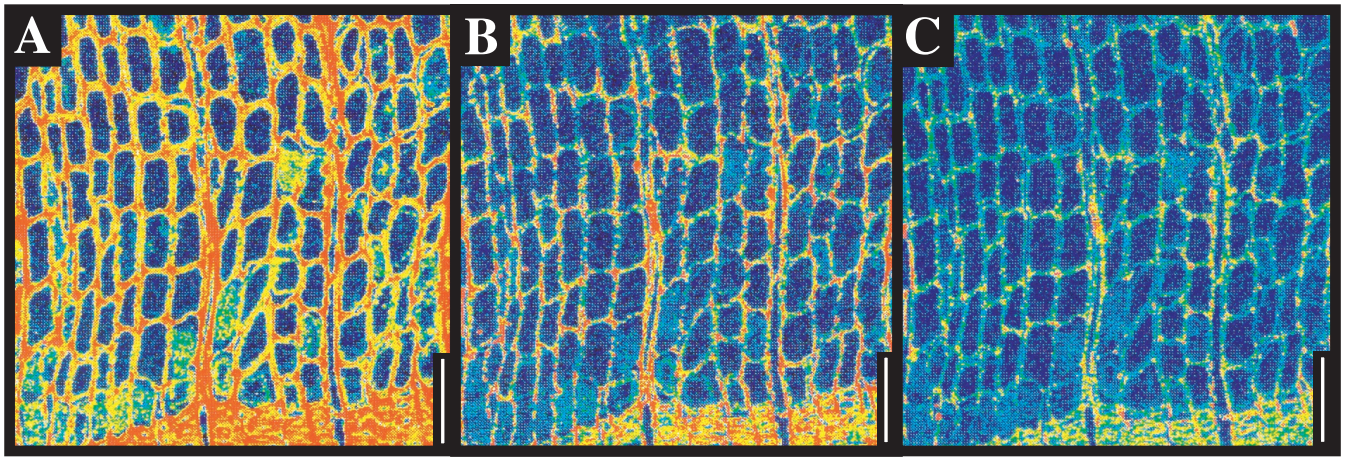

Fig. 6. Wood from the Devonian/Carboniferous Olentangy Shale. (*A*) Carbon map. (*B*) Calcium map. (*C*) Sulfur map. (Scale bars, 100 μm.)

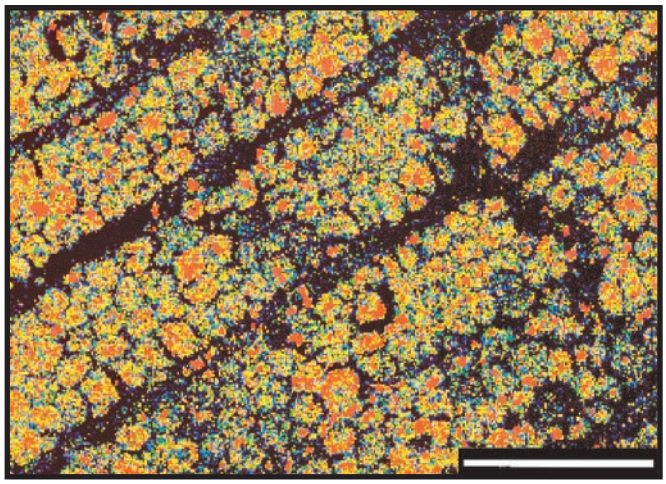

Fig. 7. Calcium map of dicot wood from the Miocene Vantage Sandstone. (Scale bar, 100 μm.)

carbonates indicates that if bacterial sulfate reduction was initiated early in diagenesis it must have been rapidly inhibited by either sulfate depletion in terrestrial ground waters or by the extensive early deposition of silica.

Silica infiltrates organic structures extensively in all samples. This may reflect the passive filling of space generated by the decay of organic material. Alternatively, silica precipitation may actively disrupt organic constituents on a submicron scale. Although complete, unaltered preservation of cell structure in three dimensions suggests that fossils were relatively robust when mineralization began, organically preserved fossils permineralized by silica are typically reduced to a fine powder by anything more than gentle etching of the fossil surface. Intact, if degraded, microfossils have on occasion been liberated by maceration from cherts, but their structural integrity cannot compare with that of superbly preserved macro and microfossils removed intact from shales (28–31). This difference suggests that silica infiltration may indeed disrupt organic fabrics on a submicron scale.

In addition to its taphonomic applications, the cellular-scale resolution and nondestructive nature of electron microprobe investigation is ideal for mapping fossils before the use of isotope ratio mass spectrometry, NMR, pyrolysis-based organic analyses, and other destructive bulk analytical methods. Within individual fossils, organic carbon is typically localized to areas appropriate for organic remnants of intact or partially degraded cell walls. However, although carbon present within the fossils is likely autochthonous, much of a sample's organic content may be dispersed in areas of high concentration in the matrix without association with an identifiable fossil source (examples in Fig. 5). Because such carbon is likely to be substantially altered or derived from allochthonous sources, bulk chemical analyses may be misleading. The electron microprobe allows one to assess the likelihood that sufficient organic material is preserved and that analyzed organics actually represent tissue-localized materials before destroying a valuable specimen. In tandem with emerging techniques for microisotopic (7) and organic geochemical analysis (32, 33), electron microprobe mapping offers the prospect of obtaining physiologically informative chemical data on specific preserved tissues and cells of ancient organisms.

Finally, little more than a decade from now, intelligently chosen rock and regolith samples are scheduled to be returned from Mars. These precious samples will be carefully analyzed for traces of past or present biological activity. The nondestructive, high resolution mapping of carbon and other co-distributed elements can provide an important first step in the astrobiological interrogation of extraplanetary materials.

We thank C. G. Hadidiacos for technical help, G. W. Rothwell for providing Princeton Chert samples, and N. H. Trewin for Rhynie Chert samples. D. Des Marais provided a helpful review of the manuscript. This research was supported in part by the National Aeronautics and Space Administration (NASA) Astrobiology Institute, a National Science Foundation predoctoral fellowship (to C.K.B.), and the Turner Foundation (R.M.H.).

1. Knoll, A. H. (1985) *Philos. Trans. R. Soc. London B* **311,** 111–122.
2. Bengtson, S. & Zhao, Y. (1997) *Science* **277,** 1645–1648.
3. Xiao, S., Zhang, Y. & Knoll, A. H. (1998) *Nature (London)* **391,** 553–558.
4. Kidston, R. & Lang, W. H. (1917) *Trans. R. Soc. Edinburgh* **51,** 761–784.
5. Remy, W., Gensel, P. G. & Hass, H. (1993) *Int. J. Plant Sci.* **154,** 35–58.
6. Edwards, D. (1993) *New Phytol.* **125,** 225–247.
7. House, C. H., Schopf, J. W., McKeegan, K. D., Coath, C. D., Harrison, T. M. & Stetter, K. O. (2000) *Geology* **28,** 707–710.
8. Hemsley, A. R., Scott, A. C., Barrie, P. J. & Chaloner, W. G. (1996) *Ann. Bot.* **78,** 83–94.
9. Edwards, D., Ewbank, G. & Abbott, G. D. (1997) *Bot. J. Linn. Soc.* **124,** 345–360.
10. Mösle, B., Collinson, M. E., Finch, P., Stankiewicz, B. A., Scott, A. C. & Wilson, R. (1998) *Org. Geochem.* **29,** 1369–1380.
11. Orr, P. J., Briggs, D. E. G. & Kearns, S. L. (1998) *Science* **281,** 1173–1175.
12. Reed, S. J. B. (1993) *Electron Microprobe Analysis* (Cambridge Univ. Press, Cambridge, U.K.).
13. Knoll, A. H. (1982) *J. Paleontol.* **56,** 755–790.
14. Kidston, R. & Lang, W. H. (1921) *Trans. R. Soc. Edinburgh* **52,** 855–902.
15. Baker, R. C. (1942) *Am. J. Sci.* **240,** 137–143.
16. Gastony, G. J. (1969) *Am. J. Bot.* **56,** 1181–1186.
17. Delevoryas, T. (1960) *Am. J. Bot.* **47,** 778–786.
18. Stockey, R. A. (1984) *Bot. Gaz.* **145,** 262–274.
19. Prakash, U. & Barghoorn, E. S. (1961) *J. Arnold Arbor.* **42,** 165–203.
20. Prakash, U. & Barghoorn, E. S. (1961) *J. Arnold Arbor.* **42,** 347–362.
21. Leo, R. F. & Barghoorn, E. S. (1976) *Bot. Mus. Leafl. Harv. Univ.* **25,** 1–46.
22. Schopf, J. M. (1975) *Rev. Palaeobot. Palynol.* **20,** 27–53.
23. Ferris, F. G., Beveridge, T. J. & Fyfe, W. S. (1986) *Nature (London)* **320,** 609–611.
24. Fortin, D., Ferris, F. G. & Scott, S. D. (1998) *Am. Mineral.* **83,** 1399–1408.
25. Wakeham, S. G., Sinninghe Damst, J. S., Kohnen, M. E. L. & de Leeuw, J. W. (1995) *Geochimica et Cosmochimica Acta* **59,** 521–533.
26. Kohnen, M. E. L., Sinninghe Damst, J. S., Kock-van Dalen, A. C., ten Haven, H. L., Rullkotter, J. & de Leeuw, J. W. (1990) *Geochimica et Cosmochimica Acta* **54,** 3053–3063.
27. Visscher, P. T., Reid, R. P. & Bebout, B. M. (2000) *Geology* **28,** 919–922.
28. Butterfield, N. J., Knoll, A. H. & Swett, K. (1994) *Fossils Strata* **34,** 1–84.
29. German, T. N. (1990) *Organic World One Billion Years Ago* (Nauka, Leningrad, Russia).
30. Gensel, P. G. (1982) *Am. J. Bot.* **69,** 651–669.
31. Grierson, J. D. & Bonamo, P. M. (1979) *Am. J. Bot.* **66,** 474–476.
32. Cody, G. D., Botto, R. E., Ade, H. & Wirick, S. (1996) *Int. J. Coal Geol.* **32,** 69–86.
33. Kudryavtsev, A., Schopf, J. W., Agresti, D. G. & Wdowiak, T. J. (2001) *Proc. Natl. Acad. Sci. USA* **98,** 823–826.